Structure of a Michaelis Complex Analogue: Propionate Binds in the Substrate Carboxylate Site of Alanine Racemase[†,‡]

Anthony A. Morollo,[§] Gregory A. Petsko,[§,||] and Dagmar Ringe*[,§,||]

Departments of Biochemistry and Chemistry and Rosenstiel Basic Medical Sciences Research Center, Brandeis University, Waltham, Massachusetts 02254

Received September 22, 1998; Revised Manuscript Received January 11, 1999

ABSTRACT: The structure of alanine racemase from *Bacillus stearothermophilus* with the inhibitor propionate bound in the active site was determined by X-ray crystallography to a resolution of 1.9 Å. The enzyme is a homodimer in solution and crystallizes with a dimer in the asymmetric unit. Both active sites contain a pyridoxal 5′-phosphate (PLP) molecule in aldimine linkage to Lys39 as a protonated Schiff base, and the pH-independence of UV−visible absorption spectra suggests that the protonated PLP−Lys39 Schiff base is the reactive form of the enzyme. The carboxylate group of propionate bound in the active site makes numerous interactions with active-site residues, defining the substrate binding site of the enzyme. The propionate-bound structure therefore approximates features of the Michaelis complex formed between alanine racemase and its amino acid substrate. The structure also provides evidence for the existence of a carbamate formed on the side-chain amino group of Lys129, stabilized by interactions with one of the residues interacting with the carboxylate group of propionate, Arg136. We propose that this novel interaction influences both substrate binding and catalysis by precisely positioning Arg136 and modulating its charge.

Biosynthesis of the peptidoglycan layer of cell walls in both Gram-positive and Gram-negative bacteria requires the addition of a D-alanine dipeptide to UDP−*N*-acetylmuramyl-L-Ala-D-Glu-*meso*-diaminopimelate. Alanine racemase (E.C. 5.1.1.1) catalyzes the racemization of the more common L-enantiomer of alanine to D-alanine, which is the substrate for D-alanine dipeptide formation by D-Ala:D-Ala ligase (E.C. 6.3.2.4). Taxonomical restriction of alanine racemase to bacteria and some fungi and the absolute requirement for D-alanine in peptidoglycan biosynthesis make alanine racemase an attractive target for inhibitors that might also function as antibiotics. Unfortunately, known inhibitors of alanine racemase are not specific as a result of mechanistic features that are common to a diverse group of PLP[1]-dependent enzymes (*1*, *2*).

Except for glycogen phosphorylase (*3*, *4*), PLP-dependent enzymes catalyze a wide variety of reactions using amino acid and amine substrates. The cofactor alone is chemically competent to catalyze many of the same basic reactions as PLP-dependent enzymes, implying that the role of the protein in a PLP-dependent holoenzyme is to control the substrate and reaction specificity of the cofactor. Proteins of at least four different classes of tertiary folds are represented among PLP-dependent enzymes, providing a remarkable example of structural convergence to common function (*1*). All of these enzymes form an imine linkage, commonly known as the internal aldimine, between the side-chain amino group of an active-site lysine residue and PLP (Scheme 1, I). The substrate amino group displaces this Schiff base in a transaldimination reaction, forming the reactive external aldimine intermediate (Scheme 1, II). Deprotonation of the α-carbon leads to the formation of an α-carbanion intermediate that is resonance-stabilized by the PLP ring (Scheme 1, III). Evidence for the existence of the resonance-stabilized α-carbanion, or quinonoid, intermediate has been obtained for a number of PLP-dependent enzymes, and the quinonoid is often invoked as a common intermediate for PLP-dependent enzymes (*1*, *2*). The simplest model for alanine racemase catalysis would involve reprotonation of the α-carbanion on either face to generate both enantiomers of alanine. Reversal of the initial transaldimination reaction then leads to product release. Understanding how alanine racemase enforces substrate and reaction specificity will require structural analysis of the Michaelis complex formed between the enzyme and its substrate, as well as the external aldimine and possibly other intermediates along the reaction pathway. This information would also promote the design of specific and effective inhibitors of the enzyme, which might also be potential antibiotics.

The structure of alanine racemase from *Bacillus stearothermophilus* was recently determined by X-ray crystallography (*5*). The polypeptide chain fold is a novel one for a PLP-containing enzyme, although it has been predicted for several other enzymes (*6*). The enzyme is a homodimer, with

[†] This work was supported by a grant from the National Science Foundation (D.R.), in part by a grant from the Lucille P. Markey Charitable Trust, and in part by National Research Service Award GM18990−02 (A.A.M.).

[‡] Coordinates have been deposited at the Brookhaven Protein Data Bank under access code 2sfp.

* Corresponding author.

[§] Rosenstiel Basic Medical Sciences Research Center.

[||] Departments of Biochemistry and Chemistry.

[1] Abbreviations: BME, β-mercaptoethanol; CAPS, 3-(cyclohexylamino)propanesulfonic acid; CHES, 2-(*N*-cyclohexylamino)ethanesulfonic acid; IPTG, isopropyl thio-β-galactoside; NAD^+, β-nicotinamide adenine dinucleotide; PEG4000, poly(ethylene glycol) 4000; PLP, pyridoxal 5′-phosphate; Tris, tris(hydroxymethyl)aminomethane; UV−vis, ultraviolet−visible.

10.1021/bi9822729 CCC: $18.00
Published on Web 02/26/1999

Scheme 1

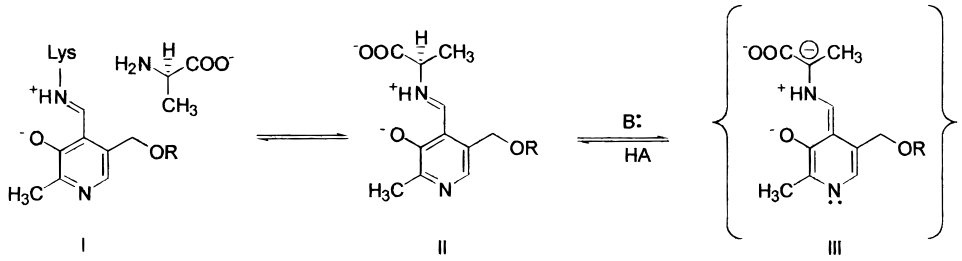

a subunit molecular mass of 43.3 kDa. Each monomer consists of an N-terminal α/β domain and a C-terminal β-strand domain, with one molecule of PLP in aldimine linkage with Lys39 at the C-terminal mouth of the α/β barrel (Figure 1). The active-site residues that bind PLP and presumably influence its function are contributed to each active site from both subunits of the dimer and are clearly delineated in this structure. Specific details of the substrate binding site are lacking due to the absence of substrate or a specific inhibitor bound to the enzyme. To define the substrate binding site for alanine and gain insight into the structure of the Michaelis complex of the enzyme, we present kinetic data showing that propionate is an effective inhibitor of *Bacillus stearothermophilus* alanine racemase and report the structure of alanine racemase with propionate bound at the active site as determined by X-ray crystallography.

EXPERIMENTAL PROCEDURES

Materials. D-Alanine, methylphosphonic acid, and ethylphosphonic acid were from Aldrich (Milwaukee, WI). PEG4000 was from Fluka Chemie AG (Buchs, Switzerland). Chromatography media and PD-10 columns were from Pharmacia (Piscataway, NJ). L-Alanine dehydrogenase was from Boehringer Mannheim (Indianapolis, IN). Centricon-10 concentrators were from Amicon (Beverly, MA).

FIGURE 1: Ribbon diagram showing an overview of the composite active site formed from contributions of both monomers. A molecule of PLP is shown in the C-terminal mouth of the α/β barrel domain of one monomer (light gray). The view shows contributions made by the β-strand domain of the other monomer (dark gray) to the active-site region. The figure was rendered with the program MolScript (*40*).

Purification. Alanine racemase from *Bacillus stearothermophilus* was purified essentially as described previously, with some modifications *(5*). *Escherichia coli* W3110 bearing the plasmid construct pMDalr3 (*7*) was grown with aeration at 37 °C in LB medium, supplemented with 100 μg/mL ampicillin, to an OD_{600} of 0.6−0.8. IPTG was added to 40 μg/mL and growth was continued for 3 h. Cells were collected by centrifugation, rinsed once with ice-cold 0.9% NaCl, and resuspended in 4 mL of buffer A (10 mM potassium phosphate, pH 7.2, 10 μM PLP, and 0.01% BME) per gram wet weight of collected cells. Cells were lysed by sonic disruption at 0 °C and the resulting lysate was cleared by centrifugation at 30000*g* for 30 min at 4 °C. The supernatant was incubated at 70 °C for 1 h and cleared by centrifugation at 20000*g* for 30 min. Solid ammonium sulfate was slowly added up to 60% saturation with continuous stirring. The precipitated protein was collected by centrifugation at 15000*g* for 20 min at 4 °C. The ammonium sulfate precipitate was resuspended in buffer A and desalted on a column of Sephadex G-25 (16 cm × 2.5 cm) equilibrated in buffer A. The protein was then loaded on a column of DEAE-Sephacel (7.5 cm × 2.6 cm) equilibrated in buffer A, washed with 4 column volumes of 20 mM KCl in buffer A, and eluted with a continuous gradient of 60−150 mM KCl in buffer A across 10 column volumes. Fractions containing alanine racemase were pooled, concentrated by ammonium sulfate precipitation, resuspended in buffer A, and exchanged into buffer B (0.5 M ammonium sulfate, 10 mM potassium phosphate, pH 7.2, 10 μM PLP, and 0.01% BME) on a column of Sephadex G-25 (16 cm × 2.5 cm) equilibrated in buffer B. The protein was loaded onto a column of phenyl-sepharose high performance (7.5 cm × 1.6 cm), washed with 5 column volumes of buffer B, and eluted with a continuous gradient to 100% buffer A in 10 column volumes followed by a wash with 5 column volumes of buffer A. Fractions containing alanine racemase were pooled. Alanine racemase was purified approximately 20-fold with a yield of 5−8 mg/L of culture. Preparations appeared as a single band when analyzed by denaturing polyacrylamide gel electrophoresis and had A_{280}/A_{420} ratios of 5.6−5.7, indicating that the protein was homogeneous with one molecule of PLP bound to each monomer (*8*).

Crystallization. Homogeneous alanine racemase was dialyzed against 2 × 1 L changes of buffer C (100 mM Tris-HCl, pH 8.5, 200 mM sodium acetate, 10 μM PLP, and 0.01% BME) and concentrated to 30 mg/mL using Centricon-10 concentrators. Hanging drops composed of 10 μL of protein solution mixed with 10 μL of well solutions (20−22% PEG4000, 200 mM sodium acetate, 10 μM PLP, 0.01% BME, and 100 mM Tris-HCl, pH 8.5) on siliconized glass cover slides were equilibrated against 700 μL of the well

Table 1: Data Collection and Refinement Statistics

Crystal Data		Refinement[c]	
space group	$P2_12_12_1$	resolution (Å)	10−1.9
unit cell parameter		reflections	49777
a (Å)	98.7	*R*-factor[d] (%)	20.5
b (Å)	90.0	R_{free} (1889 reflections) (%)	25.9
c (Å)	85.2	protein atoms	6034
$\alpha = \beta = \gamma$ (deg)	90.0	water molecules	208
Data Collection[a]		cofactor atoms	30
reflections, observed	178 589	inhibitor atoms	10
reflections, unique	52 775	*B*-factor model	individual
R_{merge}[b] (%)	5.4	restraints (rms observed)	
resolution range (Å)	30−1.9	bond length (Å)	0.01
I/σ (*I*) (average)	15.1	bond angles (deg)	1.4
completeness, overall (%)	87.0	improper angles (deg)	0.71
completeness, highest resolution shell (1.97−1.90 Å; %)	54.8	dihedral angles (deg)	27.0

[a] Using all reflections with $I/\sigma(I) > 0$. [b] $R_{merge} = \sum|I_{obs} - I_{av}|/\sum I_{av}$. [c] Using all reflections with $F/\sigma(F) > 0$. [d] *R*-factor $= \sum|F_{obs} - F_{calc}|/\sum|F_{obs}|$.

solutions in multiwell plates at ambient temperature. Individual wells were sealed with mineral oil. Crystals of alanine racemase appeared as yellow plates after 5 days and continued to form for several weeks.

Data Collection and Processing. Crystals of alanine racemase were transferred from hanging drops to a stabilizing solution [25% (w/v) PEG4000, 200 mM sodium acetate, 10 μM PLP, 0.01% BME, and 100 mM Tris-HCl, pH 8.5] and slowly exchanged over the course of several hours into a solution consisting of 25% (w/v) PEG4000, 25 mM sodium propionate, 175 mM sodium acetate, 10 μM PLP, 0.01% BME, and 100 mM Tris-HCl, pH 8.5. A single crystal (1.5 mm × 0.8 mm × 0.4 mm) was mounted in a 1.0 mM quartz capillary tube and exposed to Cu Kα radiation ($\lambda = 1.5418$ Å) at ambient temperature using a R-axis IIC image plate detector system mounted on a Rigaku RU-200 rotating anode generator operating at 45 kV and 120 mA. Data were processed with the HKL software suite (*9*). Alanine racemase crystallized in space group $P2_12_12_1$ with unit cell dimensions $a = 98.7$ Å, $b = 90.0$ Å, $c = 85.2$ Å, $a = b = c = 90°$. Statistics of the data are reported in Table 1.

Structure Refinement. The crystallographic data were refined with the program XPLOR 3.851 (*10*). Initial phases were calculated from the coordinates of unliganded alanine racemase from which PLP and waters were removed. After an initial round of positional and group *B*-factor refinement using all data between 10 and 2.5 Å, refinement was extended to 2.2 Å, at which point the *R*-factor was 26.9% and the free *R*-factor was 32.2% Electron density maps were calculated with the coefficients $2F_{obs} - F_{calc}$ and $F_{obs} - F_{calc}$ and a round of manual rebuilding was done with the program O 5.10 (*11*). Refinement was extended to 2.0 Å, electron density maps were calculated as before, and another round of manual rebuilding was performed during which a molecule of PLP was built into each monomer in aldimine linkage with Lys39 and water molecules were placed with PEAKMAX and WATPEAK from the CCP4 v3.3 package of software (*12*). Refinement was extended to 1.9 Å, after which the *R*-factor was 22.3% and the free *R*-factor was 28.0%. Rounds of water building and manual rebuilding with simulated annealing omit maps (*10*) were alternated with positional refinement, group *B*-factor refinement, and ultimately individual isotropic *B*-factor refinement using standard restraints to arrive at the final model, which consists of residues 3−381 of both monomers. Statistics of the refinement are reported in Table 1.

Steady-State Kinetic Analysis. Alanine racemase was assayed essentially as described previously (*13*). Reaction mixtures consisted of 100 mM CHES, pH 9.0, 5 mM NAD^+, 10 μM PLP, and 0.01% BME and 0.8 unit of L-alanine dehydrogenase (1 unit converts 1 μmol of L-alanine to pyruvate and NH_3 per minute at pH 10 and 25 °C), and variable concentrations of D-alanine, inhibitors, and alanine racemase as described in the Results section. Assays were performed at 37 °C in 1 mL quartz cuvettes on a Hitachi U-2000 spectrophotometer. Data were analyzed by plots as described in the text.

UV−Vis Spectroscopy. One milliliter samples of purified alanine racemase (7 mg/mL) were exchanged into various buffers by use of PD-10 columns. The following buffer systems were employed: 100 mM sodium citrate, pH 5.6, 100 mM Tris-HCl, pH 8.5, 100 mM sodium CAPS, pH 10.5, and 100 mM sodium CAPS, pH 12. Alanine racemase was collected from the columns in a single 1.5 mL fraction, with a protein concentration of 4.5 mg/mL. Spectra of the samples between 550 and 250 nm were recorded at ambient temperature in 1 mL quartz cuvettes on a Hitachi U-2000 spectrophotometer operating at a scan speed of 200 nm/min and a slit width of 2 nm.

RESULTS

The structure that we have solved from crystals soaked in sodium propionate is quite similar to the previously reported alanine racemase structure (*5*), with a mean RMS deviation of 0.29 Å on α-carbon positions and 0.86 Å for all non-hydrogen protein atoms. The final model has good geometry, with 90.3% of the residues lying in the most favored regions of the Ramachandran plot and the remaining 9.7% lying in allowed regions. The two monomers of the alanine racemase dimer have an RMS deviation of 0.24 Å for the α-carbon positions and 0.63 Å for all non-hydrogen protein atoms. Residues 163 and 289, originally identified as Leu163 and Val289, could only be built into electron density maps with poor geometry. Examination of simulated annealing omit maps (*10*) suggested that these residues were actually Val163 and Leu289, which was subsequently confirmed by DNA sequencing. Independent DNA sequencing of the alanine racemase gene from a different isolate of *Bacillus stearothermophilus* also identified Val at residue 163 and Leu at residue 289, which indicates that spontaneous mutations did not occur during the propagation of recombinant bacterial

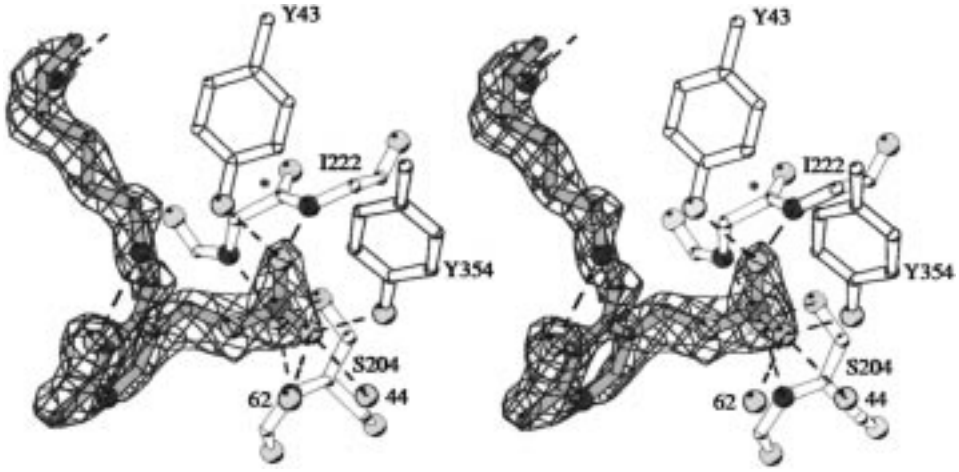

FIGURE 2: Stereo diagram of the Lys39−PLP internal aldimine viewed to show the planarity of the imine bond. The electron density shown is from a simulated annealing omit map (*10*) where atoms from Lys39 and PLP were excluded from the phase calculations. The amplitude coefficients are $2F_{obs} - F_{calc}$ and the map is contoured at 1.5 times the estimated standard deviation. Protein residues and water molecules that form the phosphate binding site are also shown. Dashed lines are drawn between potential hydrogen-bonding partners that are closer than 3.2 Å. Gly 221 is labeled with an asterisk (*) for clarity. The figure was rendered with the program MolScript (*40*).

strains (S. Sun and M. Toney, personal communication). The relevant nucleotide and amino acid sequences have been amended accordingly.

PLP is tethered to the active site by a combination of hydrogen bonds between N1 and O3 of the pyridine ring and protein residue side chains, interactions of the phosphate group with protein residue side chains and backbone amides, and a covalent bond with a lysine side chain. The NZ of Lys39 is covalently attached to the PLP cofactor in both monomers. The imine bond is essentially coplanar with the pyridine ring and the distance between NZ and O3 of PLP is 3.0 Å (Figure 2), consistent with the internally hydrogen-bonded structure anticipated for a protonated Schiff base (*14*). A deprotonated Schiff base might be expected to have the imine bond pulled almost perpendicular to the pyridine ring on the *re* face, an arrangement that has been proposed to stabilize the deprotonated form relative to the protonated form in aspartate aminotransferase, although the imine bond is pulled to the *si* face in that enzyme (*15*, *16*).

Representation of the alanine racemase internal aldimine as a protonated Schiff base is also supported by the pH independence of UV−vis absorption spectra of the internal aldimine form of the enzyme. The alanine racemase internal aldimine has been reported to have a λ_{max} at 420 nm between pH 6 and 9 (*8*). We have extended these studies and have observed a λ_{max} at 419 nm for our preparations of the enzyme between pH 5.5 and 12.0. The protonated internal aldimines of other PLP-dependent enzymes have λ_{max} values similar to the one observed for alanine racemase (*17*, *18*), while deprotonated internal aldimines have substantial blue shifts relative to the protonated species (*19*−*21*). On the basis of these considerations, we conclude that the structure we observe represents a protonated Schiff base as the keto-enamine form of the PLP cofactor.

Examination of simulated annealing omit electron density maps, which excluded the region where propionate was anticipated to bind from the phase calculations, showed electron density in the presumed substrate binding site of both subunits that can easily accommodate a molecule of propionate (Figure 3). The electron density for the C3 atom of propionate is not as strong as that for the C2 and carboxylate atoms. This may reflect a disordered (C3) methyl group, indicative of more than one binding mode for the propionate methyl group. It is also possible that the electron density represents a mixture of acetate from the crystallization buffer and propionate. Since the amount of propionate used to soak the crystals was based on previous studies (*5*) and should have been sufficient to saturate the enzyme, we decided to reexamine some of the kinetic properties of the enzyme in order to rule out the possibility that the active sites of the alanine racemase dimer are nonequivalent in solution and also to confirm the inhibition kinetics of propionate and acetate.

Steady-state kinetic analysis of alanine racemase at various fixed concentrations of acetate and propionate yielded double-reciprocal plots that intersect in the upper-left quadrant. Slope and intercept replots of the data were linear for both propionate and acetate, consistent with a mixed-type inhibition pattern, also referred to as intersecting, linear noncompetitive inhibition. Logarithmic Hill plots of the data have a slope of 1 within experimental error, indicating either that the two active sites are catalytically equivalent or that one of the active sites is catalytically silent. Slope replots indicate a K_i of 92 ± 14 mM for sodium acetate and 20 ± 3 mM for sodium propionate. These values are approximately 2.5- and 500-fold higher than those reported previously (*5*) but are consistent with a previous report of a K_i of 15 mM for propionate determined with a partially purified preparation of alanine racemase from *Pseudomonas putida* (*22*). Inhibition by short-chain carboxylic acids is quite specific. No inhibition was observed in the presence of concentrations of chloride, bicarbonate, or succinate up to 200 mM, indicating that inhibition does not arise from the interaction of general anions with a basic carboxylate binding site. We also tested the ability of the phosphonic analogues of acetate and propionate to inhibit alanine racemase. Concentrations of potassium phosphate, methylphosphonic acid, and ethylphosphonic acid up to 20 mM did not inhibit the enzyme, even when they were preincubated with the enzyme in the absence of substrate for 20 h before assays were initiated.

The specificity of inhibition by propionate allows us to unambiguously define the carboxylate binding site for the

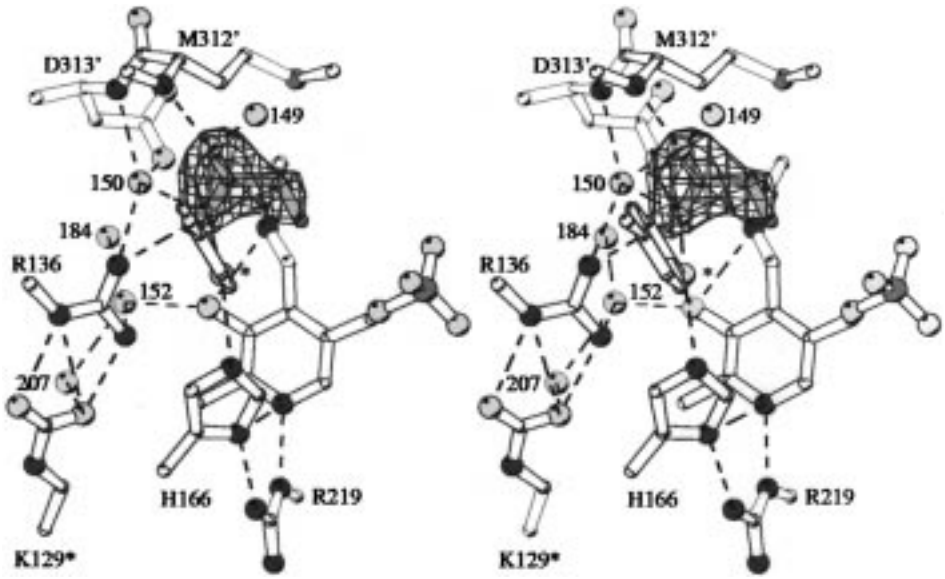

FIGURE 3: Stereo diagram of the substrate binding region. Propionate is shown built into electron density from a simulated annealing omit map (*10*) where propionate was excluded from the phases calculations. The amplitude coefficients are $2F_{obs} - F_{calc}$ and the map is contoured at 0.8 times the estimated standard deviation. Residues and water molecules which interact with N1 and O3 of the PLP ring are also shown. Lys129 is represented as a carbamate (see text). Tyr265′ is almost perpendicular with the plane of the page and is labeled with an asterisk (*) for clarity. Dashed lines are drawn between potential hydrogen-bonding partners that are closer than 3.4 Å. The figure was rendered with the program MolScript (*40*).

alanine substrate in the Michaelis complex by extension from the observed structure of propionate bound in the active site (Figure 3). The arrangement of the carboxylate binding residues is shown schematically in Figure 4. The amide N of Met 312′, which is contributed to the active site from the other subunit of the dimer, is 2.6 Å from one carboxylate oxygen (O1B) of propionate, indicating a stabilizing hydrogen bond between the amide proton and this oxygen atom. A water molecule (149) is also within hydrogen-bonding distance at 2.8 Å from O1B of propionate. The other carboxylate oxygen (O1A) of propionate is within 3.0 Å of the NH1 of Arg136, consistent with a second stabilizing hydrogen bond from that residue. The phenolic OH of Tyr265′, which is also contributed to this active site from the other subunit of the dimer, as well as a water molecule (150), are also within hydrogen-bonding distance of O1A of propionate, at 3.0 and 2.8 Å, respectively.

Arg 136 forms a bridge between O1A of propionate and a number of water molecules in the active site. In addition, NH1 of Arg136 might also form a hydrogen bond with O3 of PLP (3.6 Å). Arg136 therefore appears to be involved in carboxylate binding in a manner that is unusual in PLP-dependent enzymes, bridging the substrate and the PLP ring. In view of these observations, we believe that a critical interaction occurs between Arg136 and Lys129. The NZ of Lys129 was previously reported to interact solely with two water molecules (*5*), which would also lie within hydrogen-bonding distance of the NE and NH2 of Arg136. Modeling of this region during the early stages of refinement indicated the presence of steric clashes between the water molecules and NZ of Lys129 and NE and NH2 of Arg136. Simulated annealing omit electron density maps of this region indicated that the electron density between the NZ of Lys129 and the presumed water molecules is contiguous, even at high contour levels. We initially considered the possibility that Lys129 is an arginine residue, but DNA sequencing confirmed that the codon for this residue, an invariant lysine

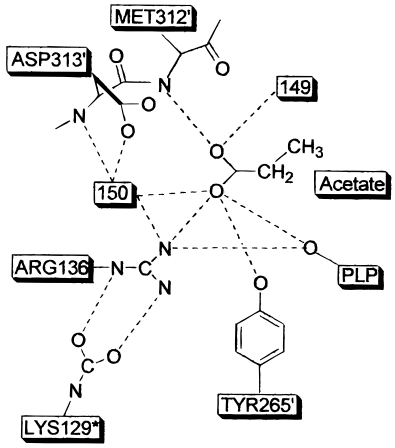

FIGURE 4: Schematic diagram of interactions made by the carboxylate group of the propionate inhibitor. Hydrogen atoms are not shown since the protonation states of all species shown are not known. Presumed hydrogen bonds are indicated by dashed lines between atoms that are separated by less than 3.6 Å. Precise distances are given in the text.

codon in alanine racemase sequences from other organisms, is also a lysine codon in the *Bacillus stearothermophilus* gene. Considering the possibility that the lysine codon might be mistranslated as arginine, we tried to build an arginine residue into the simulated annealing omit electron density map, only to find that we could do so only with poor geometry for the residue. Subsequent refinement resulted in a crest of residual density beyond the terminus of the side chain, indicating that an arginine residue is not long enough to account for the observed electron density. We therefore reasoned that a carbamate of lysine might account for the electron density that we have observed.

A carbamylated lysine was easily built into the simulated annealing omit electron density map (Figure 5) and examination of electron density maps after subsequent refinement revealed no residual difference density. The OD1 and OD2

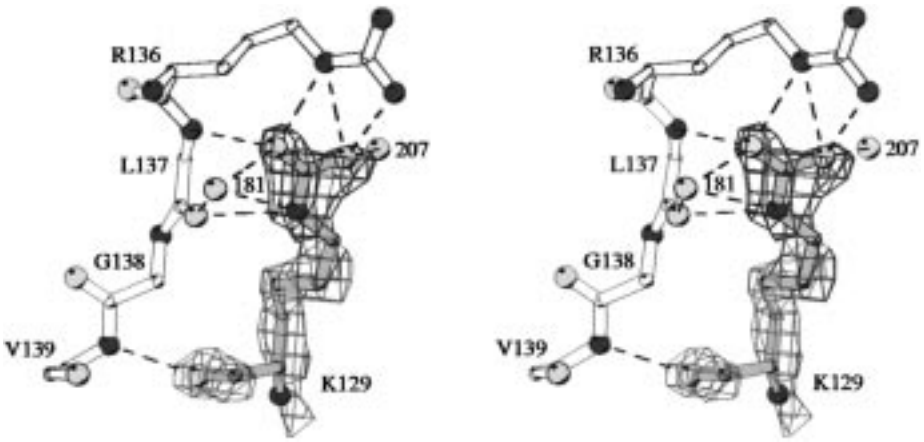

FIGURE 5: Stereo diagram of carbamylated Lys129. The lysine is shown built into electron density from a simulated annealing omit map (*10*) where Lys129 was excluded from the phase calculations. The amplitude coefficients are $2F_{obs} - F_{calc}$ and the map is contoured at 1.5 times the estimated standard deviation. Dashed lines are drawn between potential hydrogen-bonding partners that are closer than 3.4 Å. The figure was rendered with the program MolScript (*40*).

of the carbamylated lysine residue are within hydrogen-bonding distance of the NE and NH2 of Arg136, at 2.9 and 3.0 Å The *B*-factors for the side-chain NE, CZ, NH1, and NH2 atoms of Arg136 are 14.2, 15.6, 16.7, and 15.3 Å^2, respectively. These values are substantially lower than the average *B*-factor for arginine side-chain atoms for the protein as a whole (28.51 Å^2) and are quite similar to the *B*-factors for the same atoms of Arg219 (13.6, 13.9, 12.3, and 14.4 Å^2), which is in the same protein environment as Arg136 and makes numerous hydrogen-bonded contacts with its side-chain nitrogen atoms.

The active-site structure in the vicinity of N1 of the pyridine ring of PLP shows that N1 is coupled to the substrate binding site by an extended hydrogen-bonded network (Figures 3 and 4). N1 is presumably a hydrogen-bond acceptor for the protonated NE of Arg219, which is 2.9 Å away. His166 ties Arg219 to Tyr265′ through hydrogen-bonding between its ND1 and NE with NH2 of Arg219 and the phenolic O3 of Tyr265′, respectively. Tyr265′ is also within hydrogen-bonding distance of the O1A and a C2 hydrogen of propionate. The C2 carbon is in the position anticipated for the α-carbon proton of the L-enantiomer of alanine, which is destined for abstraction during catalysis. N1 of the pyridine ring is also coupled to a second extended hydrogen-bonded network by the NH1 of Arg219, which is 3.1 Å from ND1 of His200. His127 makes hydrogen bonds with the NE2 of His200 and the OE2 of Glu161 through its ND1 and NE2, respectively.

Scheme 2

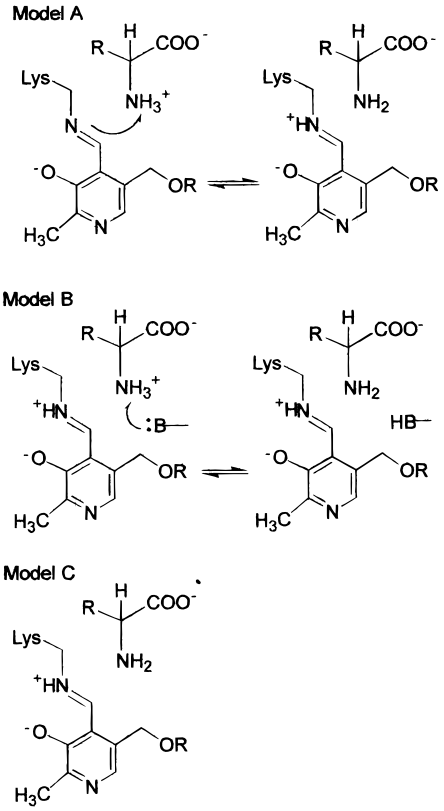

DISCUSSION

The prevailing model for catalysis by alanine racemase is summarized in Scheme 1. After formation of the Michaelis complex between the substrate and the internal aldimine form of the enzyme (Scheme 1, I), the substrate amino group displaces NZ of Lys39 in a transaldimination reaction that proceeds through a geminal diamine intermediate, leading to an external aldimine intermediate (Scheme 1, II). By analogy to other PLP-dependent enzymes, abstraction of the substrate α-proton is thought to lead to a quinonoid resonance-stabilized carbanion intermediate (Scheme 1, III), although direct evidence for the existence of the quinonoid in the alanine racemase catalytic pathway has not been observed. Protonation on the opposite side of the α-carbanion produces the other enantiomer of alanine and reprotonation on the same face regenerates the substrate. Displacement of the alanine amino group by the side-chain amino group of Lys39 through another transaldimination reaction then leads to product release.

The structure reported herein has important implications for the transaldimination step of the alanine racemase reaction, which can occur by several possible routes (Scheme 2), all of which require that a deprotonated substrate molecule attacks the imine bond to form the geminal diamine intermediate. In model A, the protonated substrate transfers a proton to the imine N of the deprotonated Schiff base, which then transaldiminates to the external aldimine form.

Model B involves a protonated substrate as well as a protonated Schiff base and invokes an enzyme base to deprotonate the substrate prior to attack on the imine bond. Model C requires that the incoming substrate is deprotonated so that it can directly attack the protonated Schiff base.

The structural and spectroscopic data described here argue against model A, which has been proposed for aspartate aminotransferase and aromatic amino acid transferase (*19*, *23*). The pK_a values of the imine nitrogen in these enzymes, approximately 6.5, would keep the enzymes largely in the deprotonated form at neutral pH and above. The high pK_a value for the alanine racemase imine nitrogen is typical of PLP-dependent enzymes other than aspartate aminotransferase and aromatic amino acid aminotransferase and would seem to ensure that the Schiff base would remain protonated at any pH relevant for catalysis. The structural data do not provide information supporting model B, in that there is no apparent enzyme base that would seem to be appropriately positioned to accept a proton from the amino acid substrate. When alanine is modeled into the binding site defined for propionate, we find that the closest contact of the alanine amino group with an enzyme base is with His166 at approximately 4.5 Å. Although we cannot rule out the possibility that conformational transitions could bring a base closer to the substrate amino group, we note that the putative enzyme base shown in model B is not suggested by X-ray crystallographic structures of other PLP-dependent enzymes (*24*−*27*). It is also conceivable that a water molecule could serve as the requisite base for model B.

A number of considerations support model C. The alkaline pH optimum for alanine racemase would ensure that the amino group of a significant fraction of the alanine substrate would be deprotonated, obviating the need to invoke an active-site base for deprotonation of the substrate. Precedents for model C are provided by *O*-acetylserine sulfhydralase (*28*, *29*) and aspartate aminotransferase, where recent work demonstrates that transaldimination occurs by the route shown in model C in addition to the historically accepted mechanism shown in model A (*30*).

The finding that in the unliganded form of alanine racemase the cofactor exists as a ketoenamine, independent of pH, is consistent with the nature of the interactions observed between active-site residues and N1 and O3 of PLP (Figure 3). The NE of Arg219 is located approximately 2.9 Å from the pyridine N1 of PLP, implying protonation of NE but not the pyridine N1. Deprotonation of the pyridine N1 would be expected to raise the pK_a of the imine nitrogen (*16*, *31*). Interactions with the O3 of PLP also influence the pK_a of the imine nitrogen. Hydrogen-bond donors to O3 decrease the pK_a of the imine, and a variety of hydrogen-bond donors interact with O3 in various PLP enzymes (*5*). The NH2 of the guanidino group of Arg136 is the closest protein atom to O3 of PLP at a distance of 3.6 Å, and the interaction of Arg136 with the carbamate of Lys129 would be anticipated to impair the ability of Arg136 to serve as a hydrogen-bond donor. A water molecule (152) is the only other potential hydrogen-bond donor to O3 of PLP at a distance of 2.6 Å. This water molecule is hydrogen-bonded only to other water molecules. The combination of the effects of interactions at N1 and O3 of PLP might be expected to contribute to the high pK_a of the imine nitrogen.

The structure of *Bacillus stearothermophilus* alanine racemase with propionate bound in the active sites unambiguously defines the carboxylate binding site of the enzyme and provides insight into the binding mode for the alanine substrate. Earlier work suggested that an acetate molecule fortuitously bound to the enzyme based on the finding that an unknown electron density observed near the NZ of Lys39 could be modeled as an acetate molecule (*5*). The inhibition constants we have measured for acetate ($K_i = 92 \pm 14$ mM) and propionate ($K_i = 20 \pm 3$ mM) establish that propionate, which approximates the size of the carbon backbone of alanine, is a superior inhibitor to acetate, with a K_i almost 5 times lower. We have also shown that inhibition by short-chain carboxylic acids is specific and is not observed when other anions are present at concentrations exceeding the K_i values for acetate and propionate. The electron density observed for propionate is neither planar nor symmetrical, allowing for unambiguous modeling of propionate in the active site (Figure 3), whereas the symmetrical density observed for acetate could accommodate three different binding modes at this resolution (*5*; A. A. Morollo and D. Ringe, unpublished data). The propionate-bound form of alanine racemase can therefore be considered to approximate many of the features of the Michaelis complex formed between the enzyme and its alanine substrate. We have modeled D-alanine and L-alanine into the active site on the basis of the coordinates of the propionate inhibitor atoms. For both enantiomers of alanine, the nitrogen atom of the α-amino group is within 3.1 Å of C4′ of PLP, appropriately positioned to initiate a transaldimination reaction with the internal aldimine.

The structure of the propionate-bound active site shows a number of features unique to alanine racemase among the PLP-dependent enzymes for which structural information exists. Enzymes such as aspartate aminotransferase (*23*), and tryptophan synthase (*24*),), dialkylglycine decarboxylase (*25*), and D-amino acid aminotransferase (*27*), typically use a single arginine group to bridge the oxygen atoms of the substrate carboxylate group. Alanine racemase uses several types of interactions to stabilize the substrate carboxylate group (Figures 3 and 4); residue side chains of Arg136 and to a lesser extent Tyr265′, the main chain of Met312′, water molecules (149 and 150), and the phenolic oxygen of PLP. It is intriguing to speculate that the carboxylate binding site of alanine racemase may be able to stabilize negative charge to a greater degree than the carboxylate binding sites of other PLP-dependent enzymes. The classical resonance-stabilized carbanion intermediate, which is invoked as a common intermediate in PLP-dependent enzymes, might not be stabilized as well by the active-site structure in the vicinity of N1 of the pyridine ring of alanine racemase, compared to the structures seen in some other PLP-dependent enzymes (*31*). The ability to propagate and stabilize some of the negative charge arising after proton abstraction from the α-carbon of the substrate into the carboxylate region might therefore be particularly advantageous for alanine racemase. It is noteworthy in this regard that the potent inhibition of the *Bacillus stearothermophilus* alanine racemase by L-alanine phosphonate has been rationalized to result from the similarity of the inhibitor to a dianionic transition state (*32*). More recently, it has been suggested that inhibition by L-alanine phosphonate is due to hydrogen-bonding interac-

tions made by the phosphate group that are not realized by a carboxylate group binding in the same site, rather than any similarity of the inhibitor external aldimine to a transition-state analogue (*33*). This model predicts that the phosphonic analogues of acetate and propionate, methylphosphonic acid and ethylphosphonic acid, should be superior inhibitors to their carboxylic acid counterparts. The absence of observed inhibition by methylphosphonic and ethylphosphonic acid relative to acetate and propionate in our experiments suggests that the additional hydrogen-bonding interactions made by the phosphate group of L-alanine phosphonate do not account for the potency of inhibition (*33*) and lend support to the dianionic transition-state model (*32*).

Carbamates of lysine have been observed by X-ray crystallography in structures of ribulose 1,5-bisphosphate carboxylase/oxygenase (*34*), urease (*35*), and phosphotriesterase (*36*). In these structures the carbamate is stabilized as a ligand to an active-site metal ion. Stopped-flow studies with glycylglycine solutions and biological tisssue extracts suggested that reaction of CO_2 with α- and ϵ-amino groups is facile and that these unprotonated amino groups form carbamates that are in equilibrium with free lysine and CO_2, albeit with the carbamate as the less abundant species (*37*). Similar studies were employed to demonstrate carbamylation of the four NH_2-terminal α-amines and 15 ϵ-amino groups of human hemoglobin (*38*). ^{13}C NMR studies have established that over 6% of the terminal α-amino groups and 2% of an internal lysine residue are carbamylated in insulin at pH 8.2 in the presence of a physiological concentration of sodium bicarbonate (*39*). The pH dependence of carbamate formation is a compromise between deprotonation of the reactive lysine, which is favored by high pH, versus the concentration of CO_2, which is favored by low pH. In the case of alanine racemase, the close proximity of Arg136 to Lys129 would be expected to promote deprotonation of the lysine. Arg136 is also perfectly positioned to stabilize the carbamate product once formed (Figure 5), in a manner similar to the way in which a metal ion stabilizes carbamates in other enzymes for which lysine carbamylation has been described (*34*−*36*), and we note that chelation of metal ions is required to disrupt the carbamates seen in these enzymes. We expect the lysine carbamate observed in alanine racemase would be a stable structure as well. The backbone amide and carbonyl of Leu137, as well as two water molecules, are also positioned to stabilize the carbamate (Figure 5). In view of the number and nature of stabilizing interactions, we expect the lysine carbamate to be a stable structure in alanine racemase.

Once the Arg136-stabilized carbamate is formed on Lys129, it would fix the position of Arg136 precisely, due to the strength of the O−N interactions. The oxygens of the lysine carbamate would be expected to carry higher partial negative charge than the cognate oxygens of a glutamate side chain due to the existence of additional resonance forms relative to glutamate. A lysine carbamate would position the oxygens approximately 1 Å closer to NE and NH1 of Arg136 than a Glu at position 129, assuming no change in the position of backbone atoms. The impact of the lysine carbamate on the interaction between Arg136 and the substrate carboxylate could be profound. The strong O−N interactions between the lysine carbamate and Arg136 would precisely position Arg136, maintaining the structural integrity of the carboxylate binding site. In the absence of the lysine carbamate, the side-chain nitrogen atoms of Arg136 would only have water molecules available as hydrogen-bonding partners.

The results presented here clarify the nature of the reactive Schiff base of alanine racemase, which has consequences for the mechanism of the transaldimination reaction, and define the carboxylate binding region of the substrate binding site. The structure also suggests that two residues might be appropriately positioned to act as bases for a proton abstraction from the alanine substrate. Lys39 is anticipated to be appropriately positioned for proton abstraction from the D-enantiomer of alanine, and Tyr265′ is appropriately positioned for proton abstraction from the L-enantiomer of alanine. Although tyrosine is not a common enzyme base, the interactions of Tyr265′ with His166 and one of the oxygen atoms of the substrate carboxylate group might be expected to lower the pK_a somewhat, bringing it closer to the pK_a for Lys39 and the pH optimum for alanine racemase, which is 9.0−9.1. Further insights into alanine racemase catalysis will be promoted by solution of the structure of an external aldimine intermediate or inhibitor structure.

ACKNOWLEDGMENT

We are grateful to Dr. Brian Bahnson for advice on data collection and Dr. Andrea Hadfield for advice on rebuilding and refinement.

REFERENCES

1. John, R. A. (1995) *Biochim. Biophys. Acta 1248*, 81−96.
2. Hayashi, H. (1995) *J. Biochem. (Tokyo) 118*, 463−473.
3. Helmreich, E. J. (1992) *Biofactors 3*, 159−172.
4. Johnson, L. N., Hu, S. H., and Barford, D. (1992) *Faraday Discuss. 93*, 131−142.
5. Shaw, J. P., Petsko, G. A., and Ringe, D. (1997) *Biochemistry 36*, 1329−1342.
6. Grishin, N. V., Phillips, M. A., and Goldsmith, E. J. (1995) *Protein Sci. 4*, 1291−1304.
7. Neidhart, D. J., Distefano, M. D., Tanizawa, K., Soda, K., Walsh, C. T., and Petsko, G. A. (1987) *J. Biol. Chem. 262*, 15323−15326.
8. Inagaki, K., Tanizawa, K., Badet, B., Walsh, C. T., Tanaka, H., and Soda, K. (1986) *Biochemistry 25*, 3268−3274.
9. Otwinowski, W., and Minor, W. (1997) *Methods Enzymol. 276*, 307−326.
10. Brünger, A. T. (1996) *X-PLOR, A system for X-ray crystallography and NMR*, Version 3.851, Yale University Press, New Haven, CT.
11. Jones, T. A., Zou, J. Y., Cowan, S. W., and Kjeldgaard, M. (1991) *Acta Crystallogr. A47*, 110−119.
12. Collaborative Computational Project 4 (1994) *Acta Crystallogr. D50*, 760−763.
13. Faraci, W. S., and Walsh, C. T. (1988) *Biochemistry 27*, 3267−3276.
14. Rhee, S., Silva, M. M., Hyde, C. C., Rogers, P. H., Metzler, C. M., Metzler, D. E., and Arnone, A. (1997) *J. Biol. Chem. 272*, 17293−17302.
15. McPhalen, C. A., Vincent, M. G., and Jansonius, J. N. (1992) *J. Mol. Biol. 225*, 495−517.
16. Okamoto, A., Higuchi, T., Hirotsu, K., Kuramitsu, S., and Kagamiyama, H. (1994) *J. Biochem. (Tokyo) 116*, 95−107.
17. Jhee, K. H., Yang, L. H., Ahmed, S. A., McPhie, P., Rowlett, R., and Miles E. W. (1998*) J. Biol. Chem. 273*, 11417−11422.
18. Demidkina, T. V., and Myagkikh, I. V. (1989) *Biochimie 71*, 565−571.
19. Ikushiro, H., Hayashi, H., Kawata, Y., and Kagamiyama, H. (1998) *Biochemistry 37*, 3043−3052.

20. Iwasaki, M., Hayashi, H., and Kagamiyama, H. (1994) *J. Biochem. (Tokyo) 115*, 156−161.
21. Goldberg, J. M., Swanson, R. V., Goodman, H. S., and Kirsch, J. F. (1991) *Biochemistry 30*, 305−312.
22. Adams, E., Mukherjee, K. L., and Dunathan, H. C. (1974) *Arch. Biochem. Biophys. 165*, 126−132.
23. Kirsch, J. F., Eichele, G., Ford, G. C., Vincent, M. G., Jansonius, J. N., Gehring, H., and Christen, P. (1984) *J. Mol. Biol. 174*, 497−525.
24. Rhee, S., Parris, K. D., Hyde, C. C., Ahmed, S. A., Miles, E. W., and Davies, D. R. (1997) *Biochemistry 36*, 7664−7680.
25. Toney, M. D., Hohenester, E., Keller, J. W., and Jansonius, J. N. (1995) *J. Mol. Biol. 245*, 151−179.
26. Sundararaju, B., Antson, A. A., Phillips, R. S., Demidkina, T. V., Barbolina, M. V., Gollnick, P., Dodson, G. G., and Wilson, K. S. (1997) *Biochemistry 36*, 6502−6510.
27. Peisach, D., Chipman, D. M., Van Ophem, P, W, Manning, J. M., and Ringe, D. (1998) *Biochemistry 37*, 4958−4967.
28. Tai, C. H., Nalabolu, S. R., Simmons, J. W., 3rd, Jacobson, T. M., and Cook, P. F. (1995) *Biochemistry 34*, 12311−12322.
29. Schnackerz, K. D., Tai, C. H., Simmons, J. W., 3rd, Jacobson, T. M., Rao, G. S., and Cook, P. F. (1995) *Biochemistry 34*, 12152−12160.
30. Hayashi, H., and Kagamiyama, H. (1997) *Biochemistry 36*, 13558−13569.
31. Yano, T., Kuramitsu, S., Tanase, S., Morino, Y., and Kagamiyama, H. (1992) *Biochemistry 31*, 5878−5887.
32. Badet, B., Inagaki, K., Soda, K., and Walsh, C. T. (1986) *Biochemistry 25*, 3275−3282.
33. Stamper. C. G. F., Morollo, A. A., and Ringe, D. (1998) *Biochemistry 37*, 10438−10445.
34. Lundqvist, T., and Schneider, G. (1991) *Biochemistry 30*, 904−908.
35. Jabri, E., Carr, M. B., Hausinger, R. P., and Karplus, P. A. (1995) *Science 268*, 998−1004.
36. Benning, M. M., Kuo, J. M., Raushel, F. M., and Holden, H. M. (1995) *Biochemistry 34*, 7973−7978.
37. Gros, G., Forster, R. E., and Lin, L. (1976) *J. Biol. Chem. 251*, 4398−4407.
38. Gros, G., Rollema, H. S., and Forster, R. E. (1981) *J. Biol. Chem. 256*, 5471−5480.
39. Griffey, R. H., Scavini, M., and Eaton, R. P. (1988) *Biophys. J. 54*, 295−300.
40. Kraulis, P. J. (1991) *J. Appl. Crystallogr. 24*, 946−950.

BI9822729